

SCALE FORMATION IN SYNTHETIC BAYER LIQUOR FOLLOWED BY QUARTZ CRYSTAL MICROBALANCE

F. Brisach¹, A. Brisach-Wittmeyer¹, N. Amokrane¹, N. A. Bouchard², H. Menard¹, and A. Lasia¹

¹ Université de Sherbrooke, Canada: Anne.Wittmeyer@USherbrooke.ca

² Rio Tinto Alcan, Arvida Research and Development Centre, Canada

ABSTRACT

The formation of fouling deposits in aluminum refining industry piping is a severe problem. In particular, these layers lead to drastic increase in heat transfer resistance and thus decrease of thermal efficiency of heat exchanger. Therefore, nucleation and growth of scale from supersaturated synthetic Bayer liquor have to be inhibited and were studied by means of a quartz crystal microbalance device (QCM) and electrochemical impedance spectroscopy (EIS). QCM, coupled with scanning electron microscopy (SEM), permitted to follow the slow deposition of aluminum trihydroxide scale particles on a gold substrate. EIS allowed collecting information on the ongoing of the early stage of nucleation in liquid phase.

Results indicate that nucleation on the gold surface of a quartz crystal gold electrode by a supersaturated aluminated solution may not occur via the commonly accepted nucleation theories. We suggest that a combination of sticking / growing and growing / sticking mechanisms of initially present particles describes the induction time before the growing period of aluminum trihydroxide layers. Use of EIS has not permitted to define exactly the events occurring but has proven that further use of this technique will contribute to the understanding of the induction period.

INTRODUCTION

The deposition of scale in pipe work and process equipment is a major issue in many industries such as metal refining (nickel, magnesium, alumina), power plants or food-processing. Sometimes scale formation may have positive effect by protecting surfaces from chemical attack or corrosion, but more often this deposit affects the performance and productivity of the process. The latter is the case in alumina refining using the Bayer process, where supersaturated solutions run in the pipes. Supersaturation in Bayer process induces precipitation of different scale type depending on the localization and the temperature of a given section of the process. For instance, during the so called "precipitation" stage, mainly gibbsite scale is involved before and in the precipitation tanks. This occurs because of the decrease of temperature from over 150 °C to around 85 °C. In some other areas where the temperature exceeds 150 °C, silica in the Bayer liquor reacts with alumina to form aluminosilicate type of scale. Half a millimeter of this kind of scale leads to 50 % decrease of thermal conductivity in less than 6 days. All these kinds of

scaling phenomena result in a decline in plant productivity whilst online and production losses when the equipment is removed from service for scale removal. Therefore, the understanding of the mechanism of nucleation and growth of scale is of major interest. Nucleation is a very slow surface coverage which happens directly onto the metallic surface at the first stage of the scaling process. Growth is a rapid crystallization of gibbsite occurring on the already deposited gibbsite. This step takes place after nucleation has finished, typically after more than 50 hours.

In our group, we developed gravimetric methods to follow scale formation by measuring mass gain as a function of time. We use several set-ups measuring mass at different scales, so scaling curves are obtained with different sensitivities (Brisach-Wittmeyer et al., 2008). Indeed, to represent the growth period, gram scale is required and only few points are necessary, although for nucleation phenomena, milligram, microgram and even nanogram scale measurements will bring more information. As our main goal is to inhibit the scaling of the industrial pipes by use of chemical or electrochemical solutions, we improved the quartz crystal microbalance (QCM) approach to make it suitable to work in Bayer liquor conditions (Gabrielli et al., 1998).

We present in this paper the first studies carried out in high caustic and supersaturated media, demonstrating that QCM can be a useful tool to follow early stages of aluminum trihydroxide scaling.

We also display first results of electrochemical impedance spectroscopy (EIS) in Bayer liquor. This technique is generally helpful when looking at the electrode / solution interface as it is the case for the early stages of nucleation phenomena.

EXPERIMENTAL CONDITIONS

Quartz crystal microbalance. The experimental set-up is described in Fig. 1. The electrochemical glass cell was thermostated by use of a Haake Fe2 heating circulator. The working electrode was a 0.5 cm diameter gold disc which is also one of the two electrodes of a 10 Mhz AT cut quartz crystal resonator. The frequency change Δf of the quartz resonator due to scale deposition on the working electrode is proportional to the mass change Δm according to the Sauerbrey relation (Sauerbrey, 1959) (1):

$$\Delta f = -C_f \Delta m \quad (1)$$

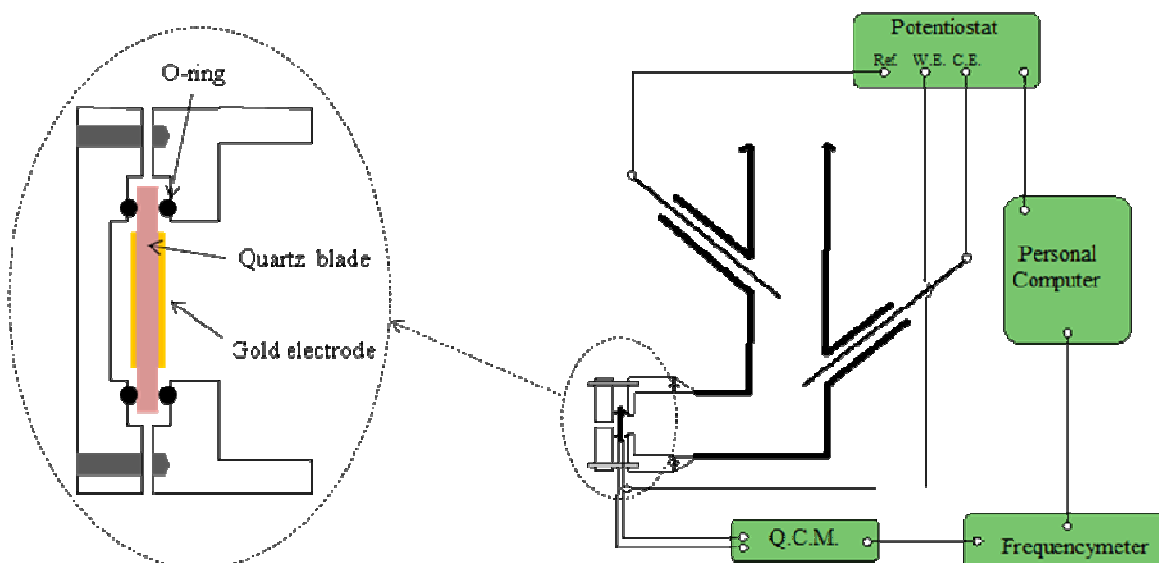


Fig. 1 Scheme of the experimental set-up used in quartz crystal microbalance frequency measurements and a zoom-in of the quartz crystal Teflon holder.

The correlation coefficient C_f is estimated by means of silver or copper electrodeposition on the working electrode and by quantifying Δm from the Faraday's law. Theoretically, $C_f = 5.4 \times 10^{-9} \text{ g cm}^{-2} \text{ Hz}^{-1}$ at 10 Mhz. In our case, no correlation between Δ_f and Δ_m has been done. When the quartz crystal resonator is inserted in the oscillator, the frequency was measured by means of a frequency counter (Agilent 53131A). Desired polarization of the working electrode was achieved by use of a potentiostat (EG&G Princeton Applied Research model 173). Pt grid and mercurous / mercurous sulphate (+ 0,929 V vs. RHE) were used as counter and reference electrodes respectively. All the experimental data were stored in a microcomputer (Hewlet Packard).

Quartz crystal resonators were purchased from ICM (Oklahoma, USA) and used as received except for 2 to 3 hours of 3M NaOH dipping.

Electrochemical impedance spectroscopy (EIS). Electrochemical impedance spectroscopy measurements were carried out using a frequency response analyzer (Solartron 1260) connected to a potentiostat (Solartron 1287) applying the desired potential. Acquisition and data processing is achieved by means of Zview software. The amplitude of the sinusoidal perturbation signal was equal to 5mV, peak to peak, in 10 khz to 100 mHz frequency range. 10 measurements points per decade were taken. A conventional three electrode cell was used with a large surface Pt grid as counter electrode and a mercurous / mercurous sulphate electrode as the reference (+ 0.929 V vs. RHE).

Scanning electron microscopy (SEM). Scale morphology was observed by scanning electron microscopy (SEM) imaging with secondary electrons or back scattered electrons (JEOL JSM-840-A, HITACHI S-3000N, HITACHI S-4700).

X-ray measurements. X-ray measurements were performed using a X'pert Pro MRD of Panalytical diffractometer with Cu K α (wavelength= 1.5406 Å) radiation.

Preparation and analysis of synthetic Bayer liquor. A synthetic supersaturated aluminate solution prepared with 180 g L⁻¹ of Al(OH)₃ (Rio Tinto Alcan), 150 g L⁻¹ of NaOH (Fisher Scientific) and 40 g L⁻¹ of Na₂CO₃ (Fisher Scientific) was used as a model for real Bayer liquor. All components were mixed together in a high-pressure vessel at 150 °C. The supersaturated aluminated solution obtained is filtered on 8 μm Whatman filter paper. Measurements of the concentration of the species in solution were done using titrimetric methods (Watts and Utley, 1953).

RESULTS

Quartz crystal resonator stability. Fig. 2 shows the frequency vs. time curve of a quartz crystal resonator in contact with 3M NaOH. The aim of this experiment was to look at the stability of the gold layer and the quartz component of the resonator in extended contact time with high caustic media, as further work will occur in synthetic Bayer liquor where caustic concentration reaches 3.75 M. The stability of the electronic part of the quartz crystal microbalance was also in concern. In 3M NaOH, 200 Hz maximum amplitude is observed over 22 hours. The main part of this value is due to thermal equilibrium that has to be reached between the sodium hydroxide solution and the coolant. This value might appear high, but in our case it is convenient because the scaling studies will involve very high frequency variations of around 250 kHz or more.

The gold deposit on the quartz crystal has only a thickness of around 1000 Å. We performed SEM imaging of an untreated and a 3M NaOH contacted quartz crystal resonators to characterize the substrate before use in scaling

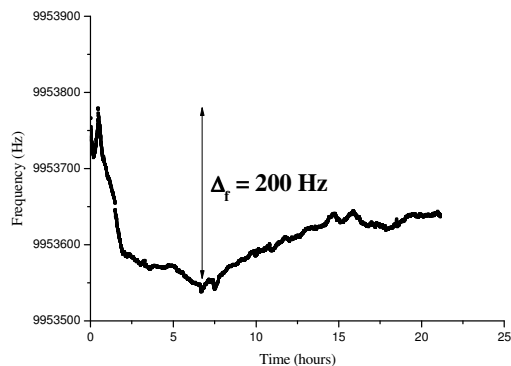


Fig. 2 QCM measurement showing the stability of a quartz crystal gold surface in 3M NaOH solution at 26 °C.

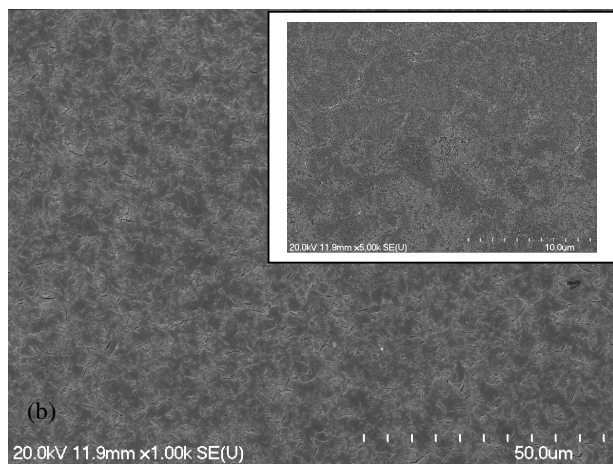
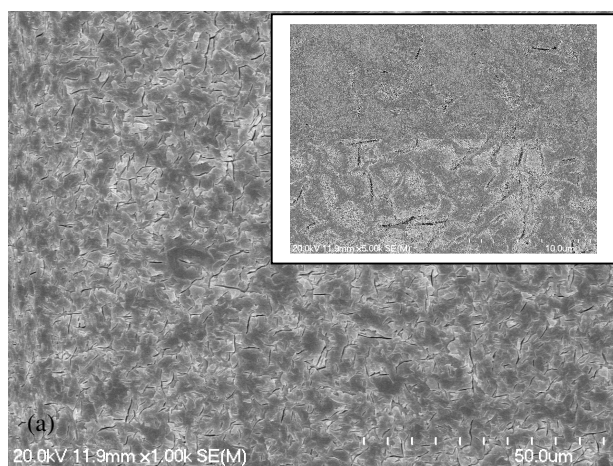


Fig. 3 SEM observation of (a) an untreated gold surface of a quartz crystal and (b) a gold surface of a quartz crystal after a 22 hours stay in 3M NaOH.

studies (Fig. 3). One can see that prolonged immersion in caustic media does not affect the gold surface of the electrodes.

Quartz crystal resonator in synthetic Bayer liquor. Once we established that stability and drift of the quartz crystal is satisfactory for our purpose, we followed the frequency variation of the electrode in contact with a slightly supersaturated synthetic aluminate solution (Fig. 4). This solution is obtained by adding gibbsite seeds to a fresh supersaturated aluminate, stirring over night and filtering.

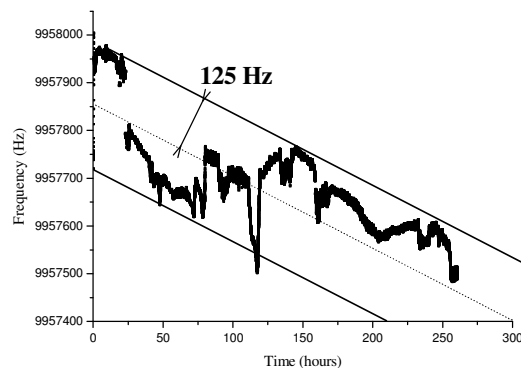


Fig. 4 QCM measurement of the stability of a quartz crystal gold surface in slightly supersaturated synthetic Bayer liquor at 26 °C.

Over an 11 days period of time, we observe a slight decrease in the frequency variations corresponding to a 50 Hz per day drift. Frequency stability of ± 125 Hz over this time period is noticed. As for the previous experiments in 3M NaOH, This very long-term stability in slightly supersaturated aluminate solution is in agreement with the results of B. R. Bickmore et al., who studied the effect of $\text{Al}(\text{OH})_4^-$ concentration on the dissolution rate of quartz (Bickmore et al., 2006). Dissolution rate of quartz decreases drastically when increasing the aluminate concentration. As in our case we use slightly supersaturated or supersaturated aluminate solution, the dissolution must be completely inhibited. This two experiments show that both quartz and gold surfaces of the quartz crystal resonator should not be affected by the caustic media, even for weeks of use.

Fig. 5 represents the frequency variations versus time during scaling on a gold electrode from a synthetic supersaturated aluminate solution. Frequency was measured every 30 s. Two different areas are characterized, one from 0 to around 60 hours and the other starting after 60 hours. During the first 60 hours of scaling, the frequency decrease is only around 10 kHz. After this period, the frequency decreases more and more quickly.

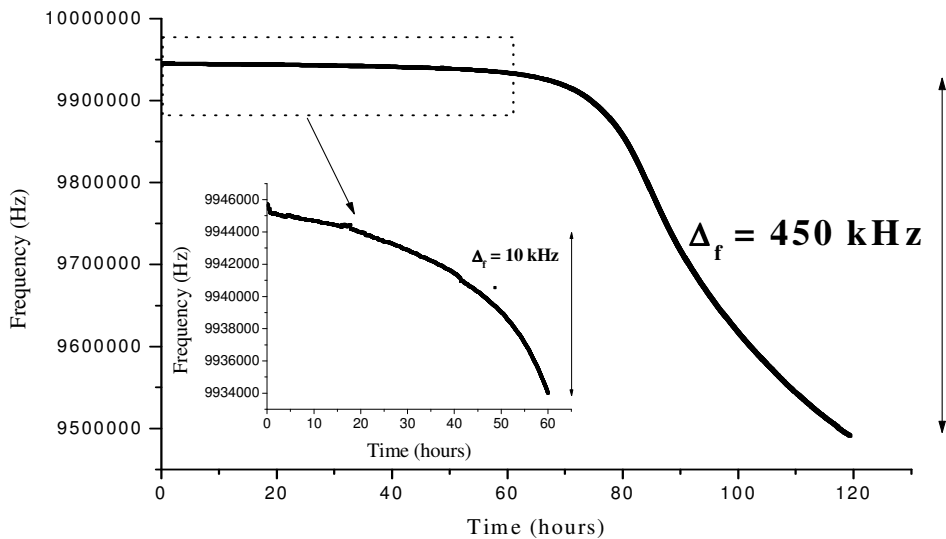


Fig. 5 QCM measurement of the scaling progress of a quartz crystal gold surface in supersaturated Bayer liquor at 26 °C.

Given the Sauerbrey relationship (1), these frequency variations are due to loading of the gold surface. We performed SEM imaging to get a view of the deposit and to correlate the frequency decrease to the morphology and the amount of deposit. Fig. 6 displays SEM images of the gold surface of several quartz crystal resonators obtained at increasing frequency losses. The first picture after 10 kHz frequency loss shows scarce particles of more than 1 μm (Fig. 6a). Elemental analysis of the surface of the electrode by Energy Dispersive X-ray Spectroscopy (EDS) gives no real evidence of presence of aluminum besides the aggregates. After 45 kHz frequency drop, much more surface is covered by aluminate particles of homogenous size around 3 μm (Fig. 6b). But uncovered gold surface is still prevailing. As for lower frequency drops, EDS analysis gives no information about presence of aluminum other than the SEM-visible fragments. At 75 kHz frequency loss, particles are again mainly monodisperse but do not recover the whole gold substrate (Fig. 6c). When reaching 100 kHz frequency decrease, $\text{Al}(\text{OH})_4^-$ free surface is reduced and particles are almost spread over the entire surface (Fig. 6d). The mean diameter of these particles is also increased at nearly 4 μm . At 220 kHz frequency drop, full surface coverage is not achieved as we can still see some rare blank areas (Fig. 6e). However, the mean diameter of the visible particles has risen up to 6 μm . Finally, after 450 kHz frequency loss or more, particles become less monodisperse and cover the whole gold surface (Fig. 6f).

We performed XRD analysis on the scale deposited on the gold substrate and results confirmed presence of bayerite and gibbsite crystal phase. This is in agreement with Lee et al. (Lee et al., 1997) that stated that bayerite is predominantly formed at room temperature while gibbsite is favored at high temperature.

DISCUSSION

This study gives evidence that a quartz crystal microbalance working in Bayer liquor conditions allows a direct evaluation of the nucleation and the crystal growth of aluminum trihydroxide on a gold substrate. Fig. 7 shows the time derivative frequency decrease corresponding to Fig. 5. One can draw a tangent line starting from the highest decrease rate point and crossing the x axis. It is accepted that the crossing point indicates the induction time of the crystal growth (El-Shall et al., 2004). We also call this period the nucleation time of scale on gold surface. In our case, nucleation period is about 70 hours.

However, in our experiment, it would be more accurate to call this 70 hours period an “apparent nucleation time”. Indeed, given the SEM observations, all the images taken at different frequency drop show monodisperse gibbsite particles. This suggests that the major part of the particles was born or present at the same time and grew at the same rate. Thus we suppose that this “apparent nucleation time” is majorly a sticking phenomenon. It is likely that aluminum trihydroxide particles, initially present in the fresh-made synthetic Bayer liquor, when colliding with the gold surface, adhere to the substrate. Therefore, two simultaneous mechanisms are coexisting, the sticking / growing or growing / sticking ones. In the first one, particles adhere to the gold surface via a cementation phenomena permitted by an $\text{Al}(\text{OH})_4^-$ interface between the gold surface and the supersaturated aluminate solution and, afterwards, grow attached to the surface. The second one proceeds the other way. Particles that grew in solution randomly collide with the quartz crystal electrode, stay stuck on the substrate via cementation and continue their growing on the gold surface. As the growing rate of particles is supposed to be the same either on the gold

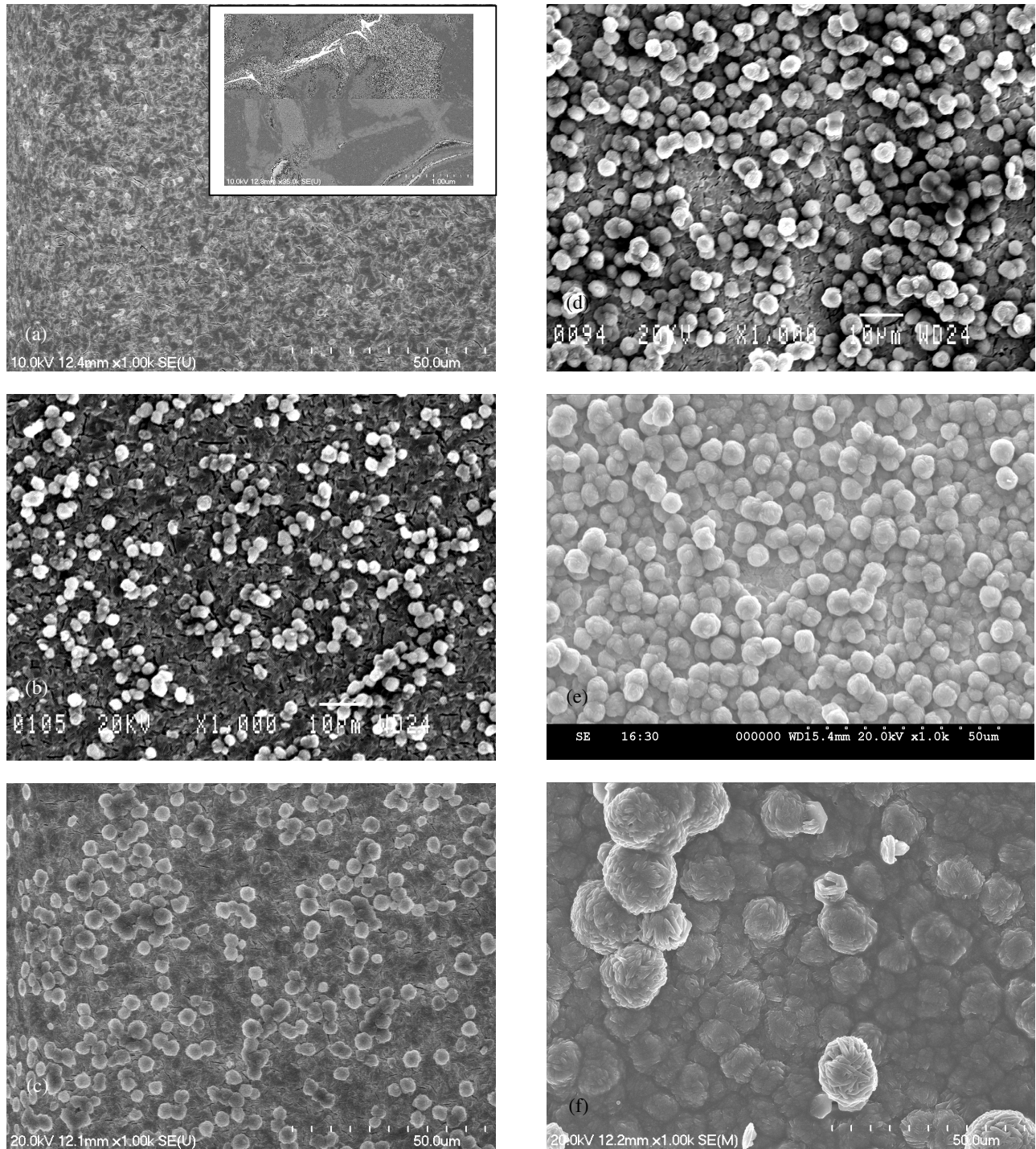


Fig. 6 SEM images of gibbsite particles and quartz crystal gold surface at increasing frequency drop (a) 10 kHz (b) 45 kHz (c) 75 kHz (d) 100 kHz (e) 220 kHz (f) 450 kHz.

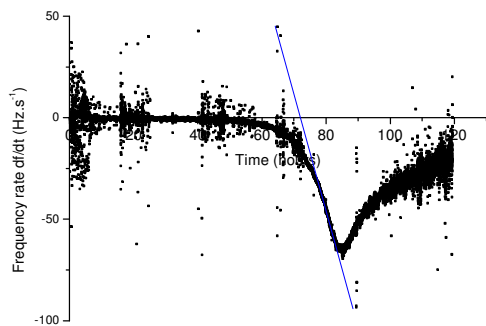


Fig. 7 Frequency rate variations while scaling of a quartz crystal gold surface from a supersaturated Bayer liquor solution.

surface or in solution, mostly monodisperse aluminum trihydroxide particles are observed.

True homogenous or heterogeneous nucleation cannot be overlooked. Nucleation is not a very well known phenomenon, but it is established that parameters such as discrete number of sites of the substrate, wetting angle between the phases, or supersaturation are of great importance (Nagy et al., 1999; Gagliano et al., 2002). As gold is not much oxidized in caustic media, relatively few oxygen atoms are present on the surface (Pourbaix, 1974). However, oxygen atoms are good anchor sites for $\text{Al}(\text{OH})_4^-$ clusters and probably are the discrete sites of the substrate. Studies involving cathodic or anodic polarization are currently under study. Anodic polarization should enhance the concentration of oxygen atoms at the gold surface by oxidizing the electrode and, on the contrary, cathodic polarization should hinder the presence of oxygen atoms. Still, this nucleation mechanism is also subject to variation in the supersaturation level of the solution. However, if the previous sticking mechanisms are consistent and proven, the latter mechanism would be hindered due to low local supersaturation induced by the growing of the already stuck particles.

SEM imaging after the 10 kHz frequency drop shows only a small amount of particles. However, the quartz crystal microbalance theory makes the assumption that the adsorbed or deposited mass is uniformly distributed over the active electrode surface (Sauerbrey, 1959). If we assume that the 10 kHz mass addition can be treated as an equivalent mass change of the quartz crystal itself, there should be a uniform foreign deposit of around 170 nm of thickness. But experimental EDS analysis does not indicate presence of aluminum atoms on the entire gold surface. We suggest that the composition of the solution at the electrode interface changes during the 70 hours period and induces these frequency variations. A nucleation mechanism for $\text{Al}(\text{OH})_3$, from unseeded concentrated sodium aluminate solutions has been proposed (Addai-Mensah et al., 2005). It is postulated that initially, $\text{NaAl}(\text{OH})_4$ ion pairs are present. As the solution ages, regions of weak polymeric networks form. As time goes on, these networks get denser. Finally, crystalline cores are formed as the densification proceeds

and growth of aluminum trihydroxide particles starts. As SEM analyses are not suited for in situ experiments, we developed an electrochemical impedance spectroscopy method to investigate the early stage of frequency drop and to distinguish between the proposed nucleation mechanisms. EIS technique involves short time polarization and gives information about the electrical double-layer at the electrode interface. Parameters like double layer capacitance, charge transfer resistance, or polarization resistance are determined. Fig. 8 presents the variations of the double layer capacitance of the quartz crystal gold electrode and the frequency drop versus time in supersaturated or slightly supersaturated aluminate solution and 3M NaOH solution. When the solution is not supersaturated, the double layer capacitance remains constant either in 3M NaOH or in slightly supersaturated aluminate solution. However, one can clearly see an increase in C_{dl} while scaling of the gold substrate goes on when the solution is supersaturated enough. This indicates that the nature or condition of the double-layer interface is changing. More studies will be necessary to conclude on what is happening to the electrode / solution interface and which nucleation mechanism is dominant.

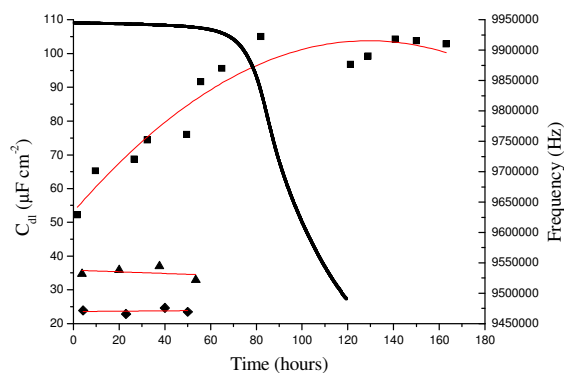


Fig. 8 Double-layer capacitance and frequency variations of a quartz crystal gold electrode in (♦) 3M NaOH (▲) slightly supersaturated aluminate solution (■) supersaturated aluminate solution.

After the induction time, growth begins and the frequency decrease rate increases quickly. As for nucleation, several mechanisms are also postulated for crystal growth, in which diffusion of species through supersaturated solution is one of the fundamental concerns. In our case, the Bayer liquor is not stirred and hence crystal growth is diffusion-driven (Mullin, 2001). Local supersaturation decreases, or even no supersaturation remains at all, and this explains why the frequency decrease rate begins to drop after 85h of scaling (Fig. 7)

CONCLUSIONS

1. This study investigates the nucleation and growth of gibbsite scale by use of quartz crystal microbalance and electrochemical impedance spectroscopy.

- For the first time, quartz crystal microbalance and electrochemical impedance spectroscopy techniques has been performed in supersaturated caustic media.
- Frequency variation over time can be used to follow the nucleation and growth of scale on gold electrode and on other metal coated electrodes like copper or iron.
- Nucleation of gibbsite on gold substrate from a synthetic supersaturated aluminate solution occurs via uncommon sticking / growing or growing / sticking mechanisms.

NOMENCLATURE

C_{dl}	double-layer capacitance, $\mu\text{F cm}^{-2}$
C_f	frequency-mass correlation coefficient, $\text{g cm}^{-2} \text{Hz}^{-1}$
Δ_f	frequency drop of quartz crystal, Hz
Δ_m	mass of deposit on quartz crystal electrode, g
EDS	Energy Dispersive X-ray Spectroscopy
EIS	Electrochemical Impedance Spectroscopy
QCM	Quartz Crystal Microbalance
RHE	Reference Hydrogen Electrode
SEM	Scanning Electron Microscopy
XRD	X-Ray Diffraction

ACKNOWLEDGMENTS

The authors want to thank Rio Tinto Alcan and the NSERC of Canada for financial support and Stephane Pelletier for the construction of the quartz crystal microbalances

REFERENCES

- A. Brisach-Wittmeyer, I. Fontaine, E. St-Jean, A. Vachon, H. Ménard, N. A. Bouchard, and R. Breault, 2008, Dynamic adsorption isotherm measurements applied to known organic precipitation inhibitors and scale control studies, *Proceedings of the 8th International Alumina Quality Workshop, Darwin, Australia*, 345-350.
- C. Gabrielli, M. Keddou, A. Khalil, G. Maurin, H. Perrot, R. Rosset, and M. Zidoune, 1998, Quartz Crystal Microbalance Investigation of Electrochemical Calcium Carbonate Scaling, *J. Electrochem. Soc.*, Vol. 145, pp. 2386-2396.
- G. Sauerbrey, 1959, Verwendung von Schwingquarzen zur Wägung dünner Schichten und zur Mikrowägung, *Z. Phys.*, Vol. 155, pp.206-222.
- H. L. Watts, and D. W. Utley, 1953, Volumetric analysis of sodium aluminate solutions, *Anal. Chem.*, Vol. 25, pp. 864-867.
- B. R. Bickmore, K. L. Nagy, A. K. Gray, and A. R. Brinkerhoff, 2006, The effect of $\text{Al}(\text{OH})_4^-$ on the dissolution rate of quartz, *Geochim. Cosmochim. Acta*, Vol. 70, pp. 290-305.
- M. Y. Lee, G. M. Parkinson, P. G. Smith, F. J. Lincoln, and M. M. Reyhani, 1997, Characterization of Aluminum Trihydroxide Crystals Precipitated from Caustic Solutions, *ACS Symposium Series*, Vol. 667, pp. 123-133.
- H. El-Shall, J-H. Jeon, E. A. Abdel-Aal, S. Khan, L. Gower, and Y. Rabinovich, 2004, A study of primary nucleation of calcium oxalate monohydrate: I-Effect of supersaturation, *Cryst. Res. Technol.*, Vol. 39, pp. 214-221.

K. L. Nagy, R. T. Cygan, J. M. Hanchar, and N. C. Sturchio, 1999, *Geochim. Cosmochim. Acta*, Vol. 63, pp. 2337-2351.

R. A. Gagliano, G. Ghosh, and M. E. Fine, 2002, Nucleation Kinetics of Cu_6Sn_5 by Reaction of Molten Tin with a Copper Substrate, *J. Electron. Mater.*, Vol. 31, pp. 1195-1202.

M. Pourbaix, 1974, *Atlas of Electrochemical Equilibria in Aqueous Solutions*, National Association of Corrosion Engineers, Houston, Texas, USA.

H. Li, J. Addai-Mensah, J. C. Thomas, and A. R. Gerson, 2005, The crystallization mechanism of $\text{Al}(\text{OH})_3$ from sodium aluminate solutions, *J. Cryst. Growth*, Vol. 279, pp. 508-520.

J. W. Mullin, 2001, *Crystallization*, 4th edition, Butterworth-Heinemann, Oxford, UK.